

Article

Effect of Modified Natural Filler *O*-Methylene Phosphonic κ -Carrageenan on Chitosan-Based Polymer Electrolytes

Joy Wei Yi Liew ¹, Kee Shyuan Loh ^{1,*}, Azizan Ahmad ², Kean Long Lim ¹ and Wan Ramli Wan Daud ^{1,3}

¹ Fuel Cell Institute, Universiti Kebangsaan Malaysia, 43600 Bangi, Selangor, Malaysia;

joy.wei yi@gmail.com (J.W.Y.L.); kllim@ukm.edu.my (K.L.L.); wramli@ukm.edu.my (W.R.W.D.)

² School of Chemical Sciences and Food Technology, Faculty of Science and Technology, Universiti Kebangsaan Malaysia, 43600 Bangi, Selangor, Malaysia; azizan@ukm.edu.my

³ Department of Chemical and Process Engineering, Faculty of Engineering and Built Environment, Universiti Kebangsaan Malaysia, 43600 Bangi, Selangor, Malaysia

* Correspondence: ksloh@ukm.edu.my; Tel.: +603-8911-8523

Received: 18 June 2018; Accepted: 6 July 2018; Published: 22 July 2018



Abstract: The potential for using *O*-methylene phosphonic κ -carrageenan (OMPk) as a filler in the chitosan-based polymer electrolyte *N*-methylene phosphonic chitosan (NMPC) was investigated. OMPk, a derivative of κ -carrageenan, was synthesized via phosphorylation and characterized using infrared spectroscopy (IR) and nuclear magnetic resonance (NMR). Both the IR and NMR results confirmed the phosphorylation of the parent carrageenan. The solid polymer electrolyte (SPE)-based NMPC was prepared by solution casting with different weight percentages of OMPk ranging from 2 to 8 wt %. The tensile strength of the polymer membrane increased from 18.02 to 38.95 MPa as the amount of OMPk increased to 6 wt %. However, the increase in the ionic conductivity did not match the increase in the tensile strength. The highest ionic conductivity was achieved with 4 wt % OMPk, which resulted in $1.43 \times 10^{-5} \text{ Scm}^{-1}$. The κ -carrageenan-based OMPk filler strengthened the SPE while maintaining an acceptable level of ionic conductivity.

Keywords: solid polymer electrolyte; chitosan; κ -carrageenan derivatives; filler; mechanical properties

1. Introduction

Solid polymer electrolytes (SPEs) have gained interest as a result of their mechanical strength, volumetric stability, solvent-free preparation, ease of production, and ability to prevent leakage in electrochemical devices compared with conventional liquid electrolytes. Most SPEs are prepared from synthetic polymers such as poly(ethylene oxide), poly(vinyl alcohol), and poly(methyl methacrylate) [1–4]. Currently, research on novel polymer use in SPEs focuses on using materials that have low production costs and are eco-friendly. Therefore, polysaccharides have been chosen as an alternative polymer because of their abundance in nature. Chitosan is one of the promising candidates among the polysaccharides to be considered as a host polymer for the preparation of SPEs. Chitosan, a linear polyaminosaccharide that is obtained by full or partial deacetylation of chitins under alkaline conditions, is known for its safety, biocompatibility, biodegradability, bioactivity, and cost-effectiveness.

The structure of chitosan contains amine and hydroxyl groups with lone pairs of electrons that can act as electron donors. However, chitosan membranes in their dry form have a very low ionic conductivity of between 10^{-9} and $10^{-10} \text{ Scm}^{-1}$ [5]. The hydrogen atoms in chitosan repeating units are strongly bonded and cannot move under the influence of an electric field. The ionic conduction that occurs in the membrane is likely due to the presence of water trapped in the membrane.

Thus, the chemical modification of chitosan was introduced to generate new functional materials with improved ionic conductivity compared to unmodified chitosan films. Most of the chemical modifications of chitosan do not change its physiochemical or biochemical properties but impart additional properties depending on the nature of the group that is introduced [6]. Chitosan can be modified as a result of the presence of reactive functional groups (NH_2 and OH) in the parent polymer. Various derivatives of chitosan have been synthesized via chemical modifications including alkylation [7], sulfonation [8], quaternary salt formation [9], and phosphorylation [10]. Even so, the use of chitosan derivatives in SPEs is still relatively unexplored. In previous studies, carboxymethyl chitosan resulted in an ionic conductivity of $3.6 \times 10^{-6} \text{ Scm}^{-1}$ at room temperature [11]. The highest recorded conductivity of a phthaloyl chitosan-based polymer electrolyte is $(2.42 \pm 0.01) \times 10^{-5} \text{ Scm}^{-1}$, which was recorded at 298 K with 30 wt % ammonium thiocyanate (NH_4SCN) [12]. These results showed that chitosan derivatives have strong potential as host polymers in SPEs, leading to investigations of phosphorylated-chitosan-based polymer electrolytes as host polymers in SPEs. The phosphorylated derivative of chitosan *N*-methylene phosphonic chitosan (NMPC) has been investigated for several biomedical applications [13–15]. NMPC was synthesized by incorporating methylene phosphonic groups into the amino groups of chitosan using formaldehyde as the coupling agent. The structure of NMPC is shown in Figure 1b. NMPC is one of the water-soluble derivatives of chitosan with anionic groups. The hydrophilic nature of chitosan-based membranes imparts poor long-term stability for applications [16]. Therefore, reinforcements from filler particles in the membrane can serve to improve both the stability and mechanical properties of the membrane.

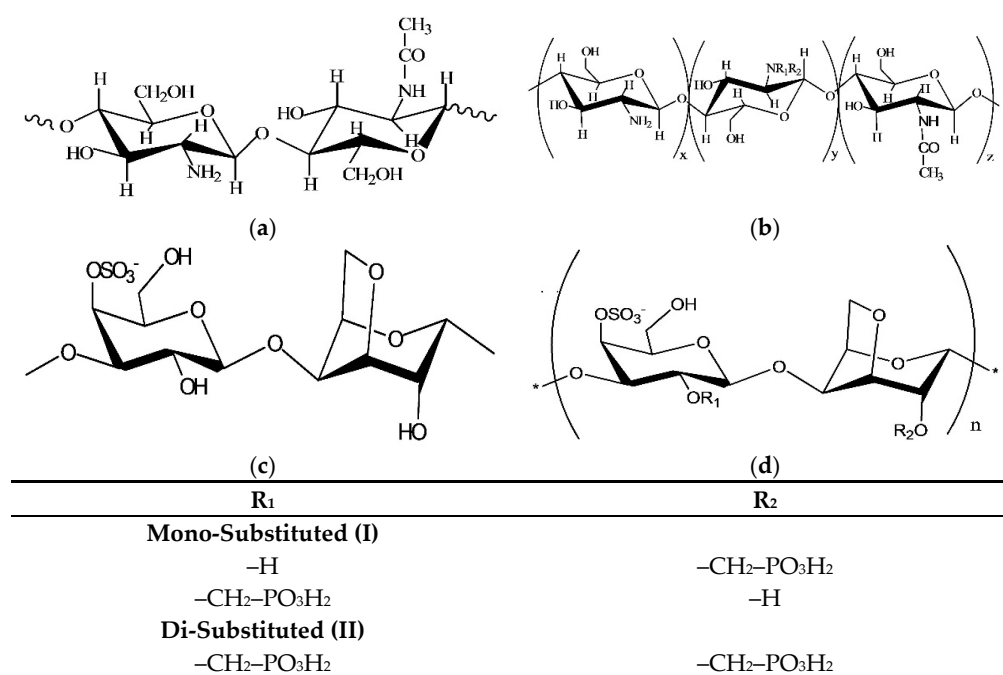


Figure 1. Molecular structure of (a) chitosan; (b) *N*-methylene phosphonic chitosan (NMPC); (c) κ -carrageenan; and (d) *O*-methylene phosphonic κ -carrageenan (OMPC).

As reported in previous studies, inorganic fillers such as SiO_2 , Al_2O_3 , ZrO_2 , and CeO_2 can be incorporated into the polymer matrix [17,18]. Synthetic fillers are non-biodegradable and will lead to waste-disposal problems. The trend in research has shifted towards using natural polymers instead. Studies on the incorporation of nanochitosan and carboxymethyl cellulose in polymer electrolytes have been reported previously [19,20]. Thus, we explored the possibility of using a κ -carrageenan-based filler. κ -Carrageenan is an anionic polymer that is extracted from the cell wall of marine red algae with repeating units of alternating (1 \rightarrow 3)- α -D-galactose-4-sulfate and (1 \rightarrow 4)- β -3,6-anhydro-D-galactose

residues. The structure of κ -carrageenan is rich in hydroxyl groups that are important for the formation of coordinate bonds with cations. *O*-Methylene phosphonic κ -carrageenan (OMPk) was synthesized using the same phosphorylation method used to produce NMPC and was introduced as a filler in the polymer matrix. The structure of OMPk is shown in Figure 1d.

Herein, we describe the synthesis of NMPC and OMPk powders. We prepared SPEs using NMPC as a polymer matrix with different weight percentages (2–8 wt %) of OMPk incorporated as the filler. The polymer electrolyte membrane was prepared using a solution casting method. The aim of this experiment was to investigate the effect of OMPk as a filler in the NMPC matrix on the electrochemical and mechanical properties of the SPE.

2. Materials and Methods

2.1. Materials

Chitosan was purchased from Sigma-Aldrich (Puchong, Selangor, Malaysia). κ -Carrageenan (TA150) was purchased from Tacara Sdn. Bhd., Tawau, Malaysia. Phosphorous acid and formaldehyde solutions were purchased from Sigma-Aldrich and were used as received (Puchong, Selangor, Malaysia). Acetic acid was purchased from Merck, and acetone was purchased from System (Puchong, Selangor, Malaysia); both were used as received. Deionized water was used throughout the experiments.

2.2. Synthesis of *N*-Methylene Phosphonic Chitosan and *O*-Methylene Phosphonic κ -Carrageenan

NMPC and OMPk were synthesized according to previously published procedures [21–24]. Chitosan or κ -carrageenan was dissolved in 1% (*v/v*) acetic acid in a three-neck round-bottom flask fitted with a reflux condenser, and the solution was heated. Once the temperature reached 60 °C, phosphorous acid was added to the solution dropwise. The temperature was raised to 70 °C, at which point formaldehyde was slowly added to the solution. The temperature was maintained between 70 and 75 °C for 8 h. After the reaction was complete, the solution was cooled, and the product was precipitated with excess acetone. The precipitate was filtered, and soxhlet extraction over the course of 24 h was used to remove unreacted phosphorous acid and formaldehyde. Finally, the product was left to dry in a desiccator.

2.3. Preparation of SPE

The membranes were prepared using a solution casting method [25,26]. NMPC (1.0 g) and different weight percentages of OMPk (2–8 wt %) were dissolved in a 1% (*v/v*) solution of acetic acid. The solution was stirred overnight. After this, OMPk was added dropwise into the NMPC solution, and the resulting solution was left to stir overnight. Afterwards, the solution was cast onto a Teflon dish and left to dry in a fume hood at room temperature until films were formed. The films were peeled off and kept in a desiccator to finish drying. Additionally, a NMPC membrane was prepared as a control by dissolving NMPC in a 1% (*v/v*) acetic acid solution. The polymer electrolyte, NMPC-OMPk, was prepared with different weight percentages of OMPk, as described in Table 1.

Table 1. Chemical composition of *N*-methylene phosphonic chitosan (NMPC)-*O*-methylene phosphonic κ -carrageenan (OMPk).

NMPC (g)/1% Acetic Acid (mL)	OMPk (wt %/g)/1% Acetic Acid (mL)
1.0/25	-
1.0/25	2/0.02/25
1.0/25	4/0.04/25
1.0/25	6/0.06/25
1.0/25	8/0/08/25

2.4. Sample Characterization

Attenuated total reflectance-Fourier transform infrared (ATR-FTIR) spectroscopy was conducted using a Nicolet 6700 (Bangi, Selangor, Malaysia) in the range of 650–4000 cm^{-1} to determine the functional groups present in the product for both the chitosan and κ -carrageenan powder. SPE membranes of different weight percentages of OMPk (2–8 wt %) were also used. Three parts of each sample were taken for the test.

^1H -NMR from a Bruker Avance III 600 MHz NMR spectrometer (Bangi, Selangor, Malaysia) was used to confirm the structures of the chitosan and κ -carrageenan derivatives. The spectra were acquired in D_2O or $\text{D}_2\text{O}/\text{CD}_3\text{COOD}$.

For thermal analysis, a thermogravimetric analysis (TGA) model STA6000 Perkin Elmer (Bangi, Selangor, Malaysia) was used to test the NMPC and NMPC-OMPk films. The samples (8–12 mg) were tested under an atmosphere of N_2 with a flow rate of 20 mL/min from ambient temperature to 700 $^\circ\text{C}$ at a heating rate of 10 $^\circ\text{C}/\text{min}$. Three parts of each sample were taken for the test.

An X-ray diffractometer, Bruker model D8 Quest SC-XRD (Bangi, Selangor, Malaysia), was used to obtain diffractograms of the SPE samples with diffraction angles, 2θ , ranging from 5 $^\circ$ to 80 $^\circ$. Three parts of each sample were taken for the test.

The tensile strength of the membrane was analyzed using an Instron 5566 (Bangi, Selangor, Malaysia) universal tensile machine. Dog-bone-shaped samples were cut from the films, which were then tested with a load cell of 50 N and a crosshead speed of 10 mm/min. The averages of five samples were taken as the results for each composition.

An electrochemical impedance spectroscopy analysis was performed at room temperature in the frequency range from 1 Hz to 1 MHz with a 10 mV amplitude using an Autolab potentiostat model AUT128N frequency response analyzer (Bangi, Selangor, Malaysia). Two probe impedance measurements were carried out with samples sandwiched between two identical stainless steel electrodes under spring pressure. The value of the conductivity, σ , was calculated using the equation $\sigma = t/(R_b A)$, where t is the film thickness (cm) measured using a hand-held micrometer, and A is the active area of the electrode (cm^2). The films' thicknesses were between 0.008 and 0.020 cm. The surface contact area of the films was 2.54 cm^2 .

3. Results and Discussion

3.1. FTIR Studies of NMPC and OMPk

To differentiate between the various chemical structures of the derivatives of chitosan and κ -carrageenan, an IR analysis was conducted. Chitosan exhibited a band at 3200–3500 cm^{-1} (Figure 2a) due to the overlapping N–H stretching and O–H stretching bands [26,27]. The characteristic peak at 1651 cm^{-1} represented the amide I band (C=O stretch of carboxamide); amide II and III bands were observed at 1591 and 1317 cm^{-1} , respectively [13,26,28]. In addition, vibrations involving C–O stretching in the chitosan skeleton appeared as strong bands at 1069 and 1028 cm^{-1} [13,27].

After phosphorylation, the IR spectrum of NMPC (Figure 2b) showed a new band at 1472 cm^{-1} due to the $-\text{CH}_2-$ bending of the methylene phosphonic unit ($-\text{CH}_2\text{PO}_3\text{H}_2$). The N–H and O–H stretching bands appeared at 3200–3500 cm^{-1} and became broader, indicating the substitution of $-\text{CH}_2\text{PO}_3\text{H}_2$ by the H atoms in the amine groups [13,29]. The shift in the amine band to a lower frequency, 1541 cm^{-1} , proved that phosphorylation occurred at the amine [13]. Additionally, the appearance of a shoulder absorbance peak at 1249 cm^{-1} was indicative of P=O stretching in the presence of the phosphate groups [24,26]. Strong bands with a high intensity appearing in the spectrum at 1070 and 1033 cm^{-1} shifted slightly to 1069 and 1028 cm^{-1} , respectively, in chitosan. These bands were attributed to the C–O stretching overlapping with the P–OH stretching [26]. On the basis of the above IR analysis, NMPC was successfully synthesized by phosphorylation. NMPC was then used as a host polymer for the SPEs.

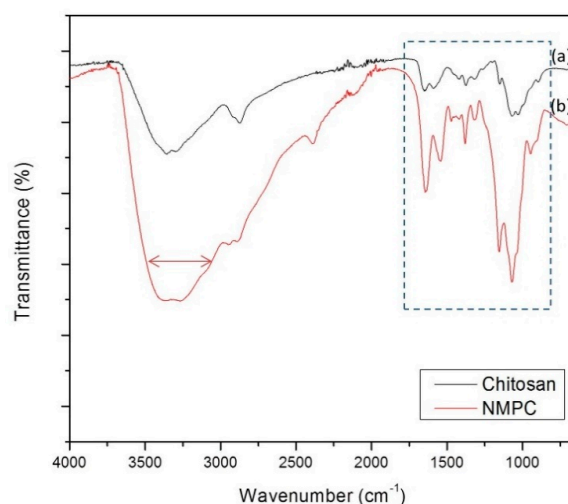


Figure 2. FTIR (Fourier transform infrared) spectra of (a) chitosan and (b) *N*-methylene phosphonic chitosan (NMPC).

In the same manner, different structural features of the κ -carrageenan derivatives could be identified from the IR analysis (Figure 3a). The absorbance bands in the κ -carrageenan IR spectrum were observed at 3407 cm^{-1} as a result of O–H stretching; at 1252 and 1230 cm^{-1} as a result of O=S=O symmetric vibrations; and at 1158 , 1069 , and 1038 cm^{-1} as a result of C–O–C stretching vibrations of the pyranose and glycosidic linkages [25,30,31]. In the IR spectrum of OMPk, as shown in Figure 3b, splitting in the O–H stretching band at 3407 cm^{-1} was observed. The band was split into peaks at 3532 and 3402 cm^{-1} , likely as a result of chemical modifications occurring at the OH group, which disturbed the κ -carrageenan structure. The hydrogen atom in the –OH functional group was replaced with $-\text{CH}_2\text{PO}_3\text{H}_2$. In addition, the absorption peak at 1682 cm^{-1} was broader and weaker because of the single OH in $\text{HO}-\text{P}=\text{O}$. In comparison with κ -carrageenan, the C–O–C stretching bands shifted to 1060 and 1033 cm^{-1} , which overlapped with the strong absorption bands at 1139 and 1121 cm^{-1} , likely as a result of P=O stretching and P–OH stretching [27,31]. The intense band from the O=S=O stretching in the κ -carrageenan spectrum shifted and became a shoulder band in the OMPk spectra at 1255 cm^{-1} because of the influence of the nearby strong absorption bands of P=O stretching and P–OH stretching. The peak shifts and the intense peak at approximately $1000\text{--}1300\text{ cm}^{-1}$ proved that changes occurred in the κ -carrageenan structure during phosphorylation.

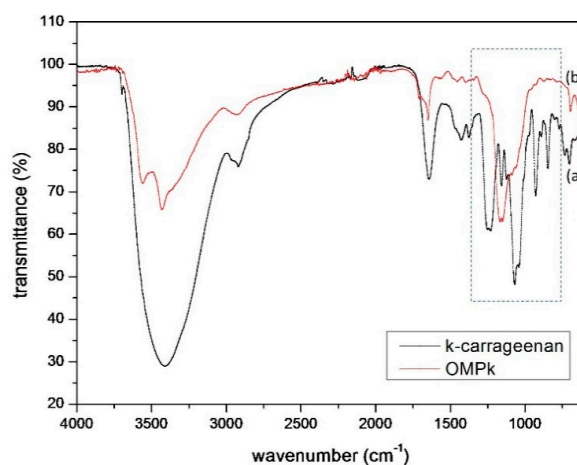


Figure 3. FTIR spectra of (a) κ -carrageenan and (b) *O*-methylene phosphonic κ -carrageenan (OMPk).

3.2. NMR Analysis of the NMPC and OMPk Powder

The ^1H -NMR spectra of chitosan and NMPC are shown in Figure 4a,b. The basic assignments of the chitosan resonances were as follows: ^1H -NMR ($\text{D}_2\text{O}/\text{CD}_3\text{COOD}$): δ 4.43 (H_1), 2.74 (H_2), 3.27–3.26 (H_3 , H_4 , H_5 , and H_6), and 1.59 ($-\text{NH}-\text{COCH}_3$). The phosphorylation of chitosan replaced the free amino group with a methylene phosphonic group ($-\text{CH}_2\text{PO}_3\text{H}_2$). Two derivatives were distinguishable in the ^1H -NMR spectrum, because two sets of peaks were observed [22]. Two additional peaks appeared at 3.06 and 2.96 ppm, which were attributed to the methylene subunit of NMPC [24]. The formation of the monophosphonic secondary amine (I) and the tertiary diphosphonic amine (II) was predicted. The spectrum showed the following chemical shifts: ^1H -NMR (D_2O): δ 7.51 (II H_1), 5.95 (I H_1), 3.27 (II H_2), 2.75 (I H_2), 3.48–4.10 (H_3 , H_4 , H_5 , and H_6), 3.06 (I- $\text{NH}-\text{CH}_2-$), 2.96 (II- $\text{N}-\text{CH}_2-$), and 1.96 ($-\text{NH}-\text{COCH}_3$).

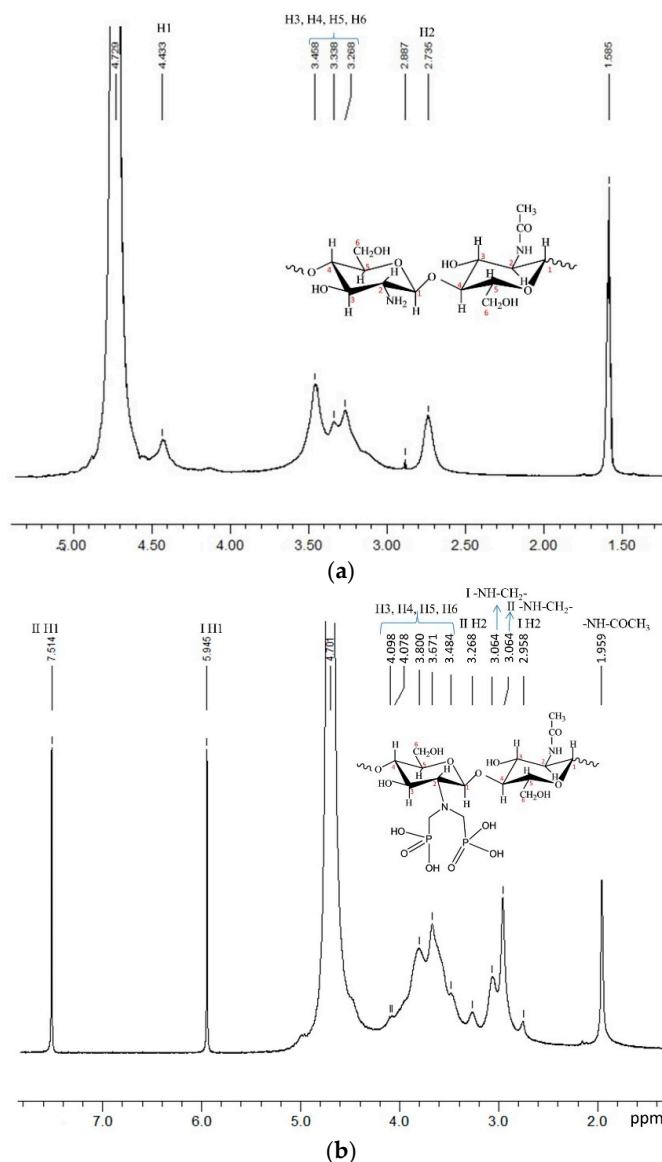


Figure 4. Nuclear magnetic resonance (NMR) spectra of (a) chitosan and (b) *N*-methylene phosphonic chitosan (NMPC).

The ^1H -NMR spectra of κ -carrageenan and OMPk are shown in Figure 5a,b. Repeating disaccharide sequences were observed in κ -carrageenan, specifically 3-linked β -D-galactopyranose

(G4S units) and 3,6-anhydro- α -D-galactopyranose (DA units). The proton assignment of the κ -carrageenan spectrum was as follows: $^1\text{H-NMR}$ (D_2O): δ 5.30 (DA-1), 3.93–3.94 (DA-2 and DA-6), 4.00 (DA-3), 4.18 (DA-4), 4.44 (DA-5), 4.95 (G4S-1), 3.52 (G4S-2), 3.86 (G4S-3), 5.18 (G4S-4), 3.65 (G4S-5), and 3.72 (G4S-6) [32–34]. The phosphorylation of κ -carrageenan was predicted to occur at the hydroxyl group, causing the hydrogen atom to be replaced with a $-\text{CH}_2\text{PO}_3\text{H}_2$ group. A new peak was observed at 3.27 ppm, which was indicative of a methylene group ($-\text{O}-\text{CH}_2-$). A shift in the H_1 of the G4S and DA units to 6.21 and 7.26 ppm, respectively, was observed. The chemical shifts arising from OMPk were assigned as follows: $^1\text{H-NMR}$ ($\text{D}_2\text{O}/\text{CD}_3\text{COOD}$): δ 7.26 (DA-1), 3.74 (DA-2 and DA-6), 3.87 (DA-3 and DA-4), 4.32 (DA-5), 6.21 (G4S-1), 3.43 (G4S-2), 3.64 (G4S-3), 5.32 (G4S-4), 3.55 (G4S-5 and G4S-6), and 3.27 ($-\text{O}-\text{CH}_2-$).

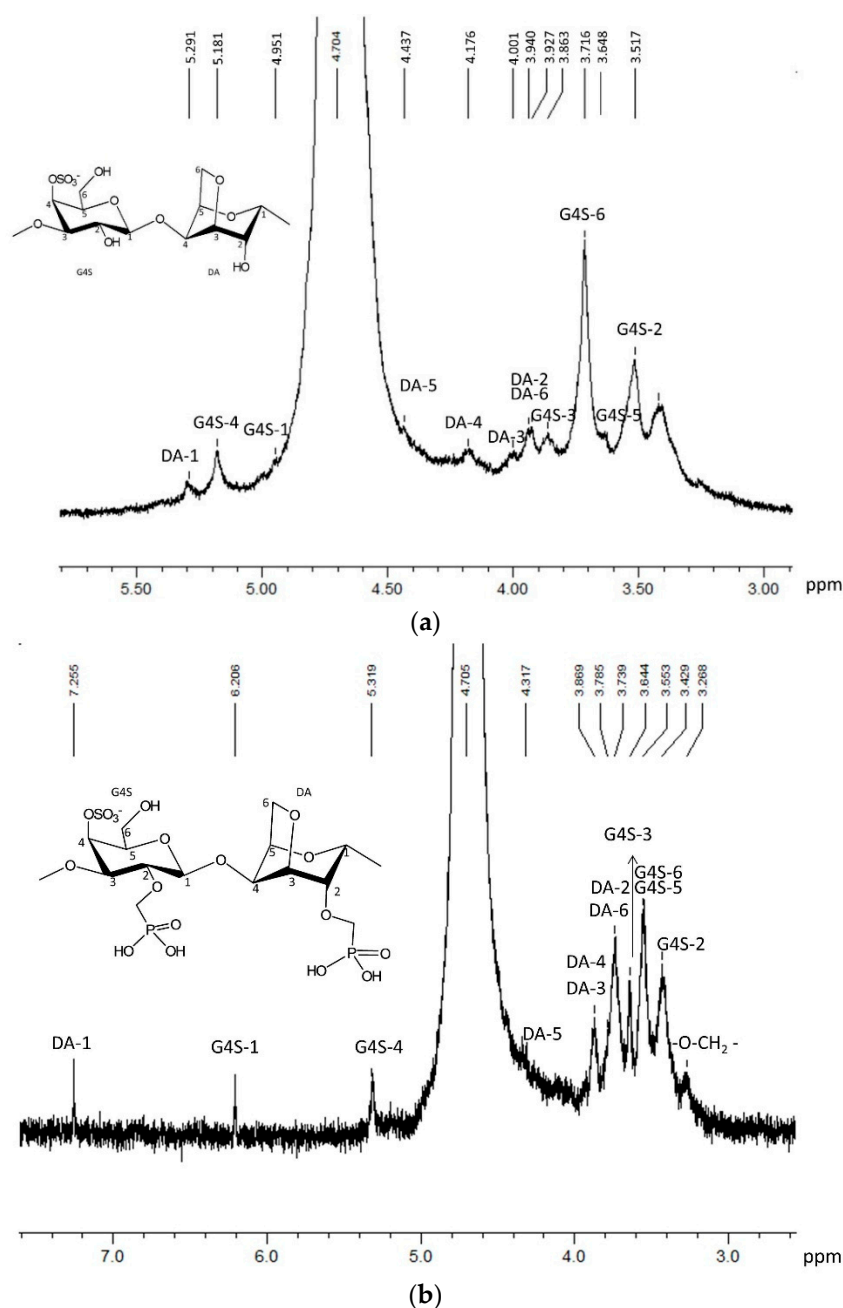


Figure 5. Nuclear magnetic resonance (NMR) spectra of the (a) κ -carrageenan and (b) O-methylene phosphonic κ -carrageenan (OMPk).

3.3. FTIR Studies of the Polymer Electrolyte Based on NMPC

The interaction between the filler and the polymer matrix was determined from the IR spectra of the NMPC-OMPk polymer electrolytes. Figure 6 shows the spectra of the NMPC and NMPC-OMPk membranes incorporated with different weight percentages of OMPk (2–8 wt %). The IR spectra of the NMPC-OMPk membranes and NMPC membranes were similar. As seen in Figure 6, a peak in the 2200–2400 cm^{-1} region was split upon the addition of the OMPk filler to the NMPC membrane. This splitting was due to the symmetric bending vibration of O=P–OH, caused by the interference of the filler with the host NMPC. In addition to splitting, the intensity of this peak increased with the increase in the amount of OMPk in the NMPC matrix due to the amount of filler causing more O=P–OH to be present in the NMPC-OMPk membranes. Overall, clear shifts in the NMPC-OMPk membranes were not observed in the IR spectra compared with the NMPC membrane. However, the IR spectra of the NMPC-OMPk membranes showed a decreased in intensity and a broadening of bands resulting from the presence of the filler [35].

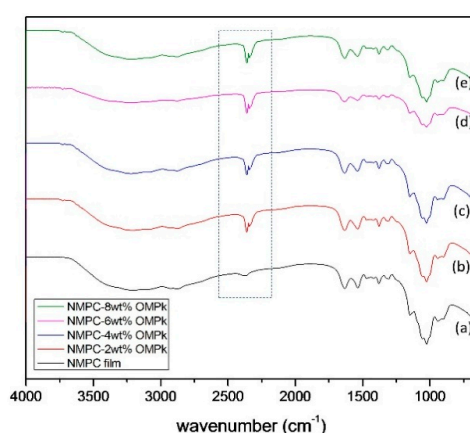


Figure 6. FTIR spectra of the solid polymer electrolytes (SPEs): (a) *N*-methylene phosphonic chitosan (NMPC) film, (b) NMPC-2 wt % *O*-methylene phosphonic κ -carrageenan (OMPk), (c) NMPC-4 wt % OMPk, (d) NMPC-6 wt % OMPk, and (e) NMPC-8 wt % OMPk.

3.4. Thermal Analysis

A thermal analysis was conducted to determine the thermal stability and behavior of the polymer. The thermograms of the NMPC and NMPC-OMPk films of various weight percentages are shown in Figure 7. The TGA curves were very similar to each other. The first common stage was below 100 °C, which was indicative of weight loss due to the removal of the absorbed water and solvent in the polymer membranes. The TGA data for the NMPC film showed a maximum degradation temperature of 221 °C as a result of the thermal decomposition of the NMPC polymer chains. For the NMPC-OMPk polymer membrane systems, the differential thermal gravimetric (DTG) curves presented one major stage of weight loss followed by a shoulder peak as the weight percentages of OMPk incorporated in the membrane increased. The major stage of weight loss occurred in the range of 170 to 245 °C as a result of the thermal decomposition of the NMPC polymer chains. The maximum degradation temperature of the NMPC-OMPk membranes was lower than that of the NMPC membranes because complexation occurred between the incorporated filler and the hydroxyl group of the polymer matrix. Hence, the loss of hydrogen bonding in the polymer matrix resulted in a lower degradation temperature [36]. Furthermore, a shoulder peak was observed at the degradation temperature region of 245–290 °C, which was likely due to the condensation reaction of the phosphonic groups with dehydration [37,38]. The DTG peaks indicated that the NMPC film was more thermally stable than the filler-filled membranes. Additionally, the weight loss of NMPC-OMPk (~30%) was larger than that of NMPC (~26%). In short, the NMPC-OMPk membrane was thermally stable up to 170 °C.

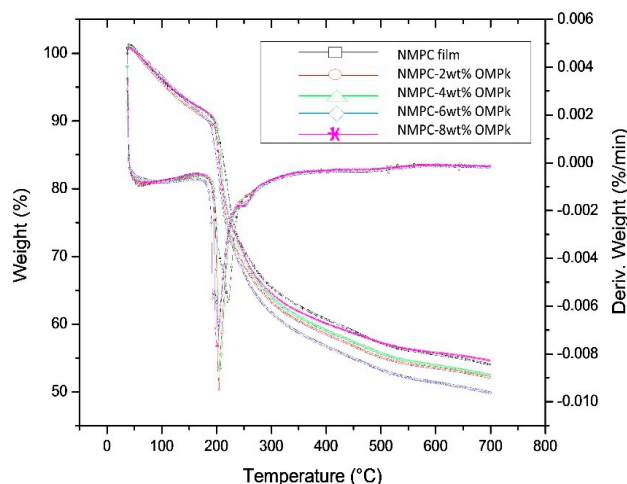


Figure 7. TGA and DTG curves of the *N*-methylene phosphonic chitosan (NMPC) film, NMPC/2 wt % *O*-methylene phosphonic κ -carrageenan (OMPk), NMPC/4 wt % OMPk, NMPC/6 wt % OMPk, and NMPC/8 wt % OMPk.

3.5. X-ray Diffraction (XRD) Studies

X-ray diffraction (XRD) studies were used to analyze the effect of filler addition to the polymer matrix on the degree of crystallinity of the polymer electrolyte samples. The XRD diffractograms in Figure 8 show that both the NMPC polymer electrolyte and the NMPC-OMPk polymer electrolyte system existed in an amorphous or semi-crystalline phase. As shown, a broad hump appeared in the range of 2θ of 10° to 30° for the NMPC film, which was attributed to an amorphous phase. However, the reinforcement of OMPk in the NMPC polymer host resulted in a significant increase in the degree of crystallinity of the membrane in the region of 2θ of 15° to 30° as the hump became narrower compared with that of the pure NMPC film. Thus, the filler-filled membranes were in a semi-crystalline phase. The magnitudes of the peaks with 2 and 4 wt % OMPk were identical. In comparison, the magnitudes of the peaks with 6 and 8 wt % OMPk were similar to each other and had higher intensities than the 2 and 4 wt % peaks. The higher intensity peaks indicated a higher degree of crystallinity in the membrane. In addition, the improvement in the crystallinity of the NMPC-OMPk membranes enhanced the mechanical properties of the SPE films.

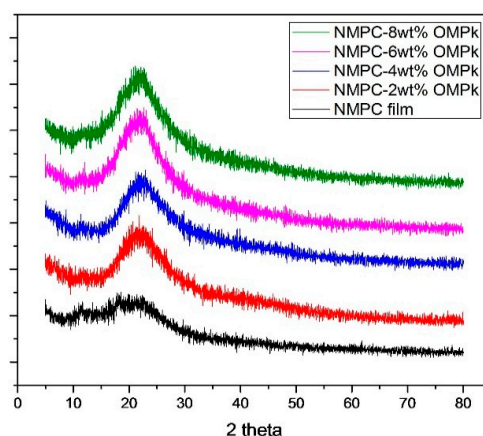


Figure 8. X-ray diffraction (XRD) diffractograms of the *N*-methylene phosphonic chitosan (NMPC) film, NMPC/2 wt % *O*-methylene phosphonic κ -carrageenan (OMPk), NMPC/4 wt % OMPk, NMPC/6 wt % OMPk, and NMPC/8 wt % OMPk.

3.6. Mechanical Properties

The mechanical properties of SPEs are related to the processing method, the compatibility of the filler and polymer matrix, and the filler-filler interactions. In this case, the incorporation of OMPk in NMPC improved the overall mechanical properties of the polymer electrolyte membrane because the filler particles acted as a support matrix for the conductive polymer electrolytes to retain an overall solid structure, even at higher temperatures. The accuracy of the tensile strength was determined in accordance with the results shown in Figure 9. This is indicated by the error bars. In general, the tensile strength of the NMPC-OMPk films was better than that of the NMPC films. The NMPC films had a tensile strength of 18.02 MPa. The tensile strength initially increased with the increasing OMPk content and reached an optimum value of 38.95 MPa at 6 wt % OMPk before subsequently decreasing. The high value of the tensile strength of NMPC/6 wt % OMPk was in accordance with the high crystallinity in the SPE system [39]. With a greater amount of OMPk, the poor particle distribution in the NMPC matrix caused the filler particles to agglomeration, decreasing the tensile strength [39,40]. Overall, the SPE with the filler exhibited a much higher tensile strength than the membrane without the filler.

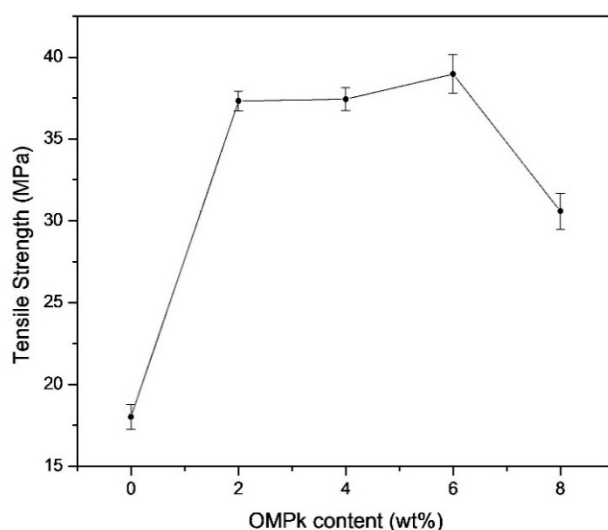


Figure 9. Graph of the tensile strength with respect to the *O*-methylene phosphonic κ -carrageenan (OMPk) content.

3.7. Ionic Conductivity

From the electrochemical impedance spectroscopy (EIS) analysis, the ionic conductivity of the NMPC membrane at room temperature was $3.56 \times 10^{-6} \text{ Scm}^{-1}$, which was approximately 3 orders of magnitude higher than the values reported for chitosan membranes in the literature [5]. Increasing the number of oxygen atoms present in NMPC relative to those in chitosan changed the conductive properties of the polymer [11]. In other words, the increase in the number of active sites per repeating unit in the polymer enhanced the migration of protons through the polymer matrix by providing more vacant sites for proton transport to occur. Thus, an improvement in the ionic conductivity resulted from the amelioration of proton transportation. The change in the ionic conductivity with respect to the change in the amount of incorporated OMPk in the composite electrolyte membrane is shown in Figure 10. This is indicated by the error bars as an accuracy measurement.

As the amount of filler added to the electrolyte polymer increased, the ionic conductivity increased until it reached a maximum of $1.43 \times 10^{-5} \text{ Scm}^{-1}$ at 4 wt % OMPk, as recorded at room temperature. The improvement in the ionic conductivity was likely due to the anion sites in the filler coordinating with the protons in the sample, which provided a new conduction pathway for proton hopping and exchange to occur in the NMPC membrane. From the EIS analysis data, further addition of the filler

above 4 wt % OMPk caused a decrease in the ionic conductivity of the polymer electrolyte. As in previous reports, with further addition of the filler after reaching saturation, the conductivity decreased because of a blocking effect imposed by the more abundant OMPk. The long polymer chains were “immobilized” and caused the conductivity to decrease [41]. The decrease may have also been due to the interactions between the polymer matrix and the filler through coordination bonds causing a decrease in the free space for proton conduction to occur.

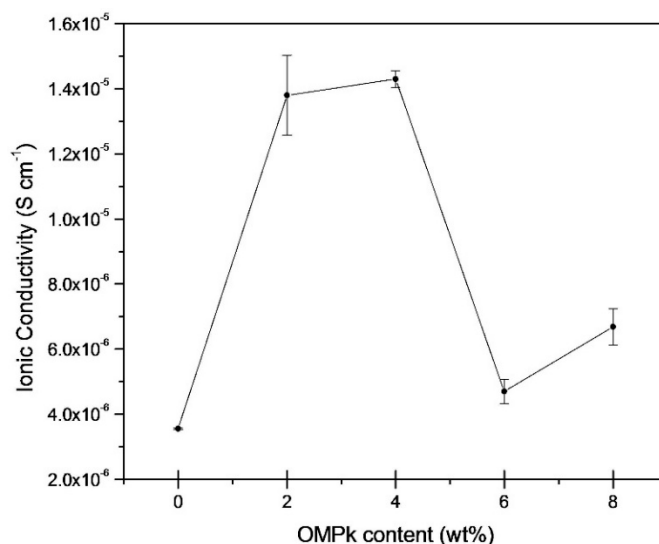


Figure 10. Graph of the ionic conductivity of the solid polymer electrolyte (SPE) with respect to the *O*-methylene phosphonic κ -carrageenan (OMPk) content in *N*-methylene phosphonic chitosan (NMPC).

4. Conclusions

In conclusion, the modification of chitosan and κ -carrageenan was observed through FTIR and ¹H-NMR analysis. Methylene phosphonic groups were introduced in the chitosan structure and enhanced the ionic conductivity of the biopolymer electrolyte. Overall, the new derivative of κ -carrageenan, which acted as a filler in the polymer electrolyte system, greatly improved the mechanical strength of the SPE, even when a small amount of OMPk was added. For further improvement, the design of a new SPE with a high ionic conductivity and better mechanical strength may be achieved by blending with other polymers.

Author Contributions: The listed authors contributed to this work as follows: K.S.L. and A.A. conceived and designed the experiments; J.W.Y.L. performed the experiments and prepared the manuscript; J.W.Y.L. and K.L.L. analyzed the data; K.S.L. and W.R.W.D. contributed reagents/materials/analysis tools.

Funding: This research received funding from the Universiti Kebangsaan Malaysia (UKM) through the University Research Grants DPP-2018-003 and GUP-2016-038.

Acknowledgments: The authors would like to acknowledge the support of human capital development given by the Malaysia Ministry of Higher Education.

Conflicts of Interest: The authors declare no conflict of interest. The founding sponsors had no role in the design of the study; in the collection, analyses, or interpretation of data; in the writing of the manuscript; or in the decision to publish the results.

References

1. Rajendran, S.; Sivakumar, M.; Subadevi, R. Investigations on the effect of various plasticizers in PVA–PMMA solid polymer blend electrolytes. *Mater. Lett.* **2004**, *58*, 641–649. [\[CrossRef\]](#)
2. Wu, G.M.; Lin, S.J.; Yang, C.C. Preparation and characterization of PVA/PAA membranes for solid polymer electrolytes. *J. Membr. Sci.* **2006**, *275*, 127–133. [\[CrossRef\]](#)

3. Rajendran, S.; Mahendran, O. Experimental investigations on plasticized PMMA/PVA polymer blend electrolytes. *Ionics* **2001**, *7*, 463–468. [[CrossRef](#)]
4. Ramesh, S.; Winie, T.; Arof, A.K. Investigation of mechanical properties of polyvinyl chloride–polyethylene oxide (PVC–PEO) based polymer electrolytes for lithium polymer cells. *Eur. Polym. J.* **2007**, *43*, 1963–1968. [[CrossRef](#)]
5. Wan, Y.; Creber, K.A.M.; Peppley, B.; Bui, V.T. Ionic conductivity of chitosan membranes. *Polymer* **2003**, *44*, 1057–1065. [[CrossRef](#)]
6. Jiang, M.; Wang, K.; Kennedy, J.F.; Nie, J.; Yu, Q.; Ma, G. Preparation and characterization of water-soluble chitosan derivative by Michael addition reaction. *Int. J. Biol. Macromol.* **2010**, *47*, 696–699. [[CrossRef](#)] [[PubMed](#)]
7. Yang, T.-C.; Chou, C.-C.; Li, C.-F. Preparation, water solubility and rheological property of the N-alkylated mono or disaccharide chitosan derivatives. *Food Res. Int.* **2002**, *35*, 707–713. [[CrossRef](#)]
8. Jayakumar, R.; Nwe, N.; Tokura, S.; Tamura, H. Sulfated chitin and chitosan as novel biomaterials. *Int. J. Biol. Macromol.* **2007**, *40*, 175–181. [[CrossRef](#)] [[PubMed](#)]
9. De Britto, D.; Assis, O.B.G. A novel method for obtaining a quaternary salt of chitosan. *Carbohydr. Polym.* **2007**, *69*, 305–310. [[CrossRef](#)]
10. Matevosyan, G.L.; Yukha, Y.S.; Zavlin, P.M. Phosphorylation of chitosan. *Russ. J. Gen. Chem.* **2003**, *73*, 1725–1728. [[CrossRef](#)]
11. Mobarak, N.N.; Ahmad, A.; Abdullah, M.P.; Ramli, N.; Rahman, M.Y.A. Conductivity enhancement via chemical modification of chitosan based green polymer electrolyte. *Electrochim. Acta* **2013**, *92*, 161–167. [[CrossRef](#)]
12. Aziz, N.A.; Majid, S.R.; Arof, A.K. Synthesis and characterizations of phthaloyl chitosan-based polymer electrolytes. *J. Non-Cryst. Solids* **2012**, *358*, 1581–1590. [[CrossRef](#)]
13. Datta, P.; Dhara, S.; Chatterjee, J. Hydrogels and electrospun nanofibrous scaffolds of N-methylene phosphonic chitosan as bioinspired osteoconductive materials for bone grafting. *Carbohydr. Polym.* **2012**, *87*, 1354–1362. [[CrossRef](#)]
14. Zhu, D.; Yao, K.; Bo, J.; Zhang, H.; Liu, L.; Dong, X.; Song, L.; Leng, X. Hydrophilic/lipophilic N-methylene phosphonic chitosan as a promising non-viral vector for gene delivery. *J. Mater. Sci. Mater. Med.* **2010**, *21*, 223–229. [[CrossRef](#)] [[PubMed](#)]
15. Rodriguez, M.S.; Albertengo, L.; Etcheverry, M.; Schulz, P.C. Studies on N-methylene phosphonic chitosan. *Colloid Polym. Sci.* **2005**, *283*, 1298–1304. [[CrossRef](#)]
16. Saxena, A.; Kumar, A.; Shahi, V.K. Preparation and characterization of N-methylene phosphonic and quaternized chitosan composite membranes for electrolyte separations. *J. Colloid Interface Sci.* **2006**, *303*, 484–493. [[CrossRef](#)] [[PubMed](#)]
17. Pandey, G.P.; Hashmi, S.A.; Agrawal, R.C. Hot-press synthesized polyethylene oxide based proton conducting nanocomposite polymer electrolyte dispersed with SiO₂ nanoparticles. *Solid State Ion.* **2008**, *179*, 543–549. [[CrossRef](#)]
18. Aravindan, V.; Vickraman, P. Polyvinylidene fluoride–hexafluoropropylene based nanocomposite polymer electrolytes (NCPE) complexed with LiPF₃(CF₃CF₂)₃. *Eur. Polym. J.* **2007**, *43*, 5121–5127. [[CrossRef](#)]
19. Balakumar, S.; Shajan, X.S. Structural and ionic conductivity studies on nanochitosan incorporated polymer electrolytes for rechargeable magnesium batteries. *Chem. Sci. Trans.* **2012**, *1*, 311–316.
20. Jafirin, S.; Ahmad, I.; Ahmad, A. Carboxymethyl cellulose from kenaf reinforced composite polymer electrolytes based 49% poly (methyl methacrylate)-grafted natural rubber. *Malays. J. Anal. Sci.* **2014**, *18*, 376–384.
21. Ramos, V.M.; Rodriguez, N.M.; Rodriguez, M.S.; Heras, A.; Agullo, E. Modified chitosan carrying phosphonic and alkyl groups. *Carbohydr. Polym.* **2003**, *51*, 425–429. [[CrossRef](#)]
22. Heras, A.; Rodríguez, N.M.; Ramos, V.M.; Agulló, E. N-methylene phosphonic chitosan: A novel soluble derivative. *Carbohydr. Polym.* **2001**, *44*, 1–8. [[CrossRef](#)]
23. Binsu, V.V.; Nagarale, R.K.; Shahi, V.K.; Ghosh, P.K. Studies on N-methylene phosphonic chitosan/poly(vinyl alcohol) composite proton-exchange membrane. *React. Funct. Polym.* **2006**, *66*, 1619–1629. [[CrossRef](#)]
24. Zhao, D.; Xu, J.; Wang, L.; Du, J.; Dong, K.; Wang, C.; Liu, X. Study of two chitosan derivatives phosphorylated at hydroxyl or amino groups for application as flocculants. *J. Appl. Polym. Sci.* **2012**, *125*, E299–E305. [[CrossRef](#)]

25. Mobarak, N.N.; Ramli, N.; Ahmad, A.; Rahman, M.Y.A. Chemical interaction and conductivity of carboxymethyl κ -carrageenan based green polymer electrolyte. *Solid State Ion.* **2012**, *224*, 51–57. [[CrossRef](#)]
26. Amaral, I.F.; Granja, P.L.; Barbosa, M.A. Chemical modification of chitosan by phosphorylation: An XPS, FT-IR and SEM study. *J. Biomater. Sci. Polym. Ed.* **2005**, *16*, 1575–1593. [[CrossRef](#)] [[PubMed](#)]
27. Fadzallah, I.A.; Majid, S.R.; Careem, M.A.; Arof, A.K. A study on ionic interactions in chitosan–oxalic acid polymer electrolyte membranes. *J. Membr. Sci.* **2014**, *463*, 65–72. [[CrossRef](#)]
28. Smitha, B.; Sridhar, S.; Khan, A.A. Chitosan–sodium alginate polyion complexes as fuel cell membranes. *Eur. Polym. J.* **2005**, *41*, 1859–1866. [[CrossRef](#)]
29. Wang, Q.; Chen, J.; Huang, K.; Zhang, X.; Xu, L.; Shi, Z.-G. Preparation, characterization and application of N-methylene phosphonic acid chitosan grafted magnesia–zirconia stationary phase. *Anal. Chim. Acta* **2015**, *854*, 191–201. [[CrossRef](#)] [[PubMed](#)]
30. Tranquilan-Aranilla, C.; Nagasawa, N.; Bayquen, A.; Dela Rosa, A. Synthesis and characterization of carboxymethyl derivatives of kappa-carrageenan. *Carbohydr. Polym.* **2012**, *87*, 1810–1816. [[CrossRef](#)]
31. Ma, S.; Chen, L.; Liu, X.; Li, D.; Ye, N.; Wang, L. Thermal behavior of carrageenan: Kinetic and characteristic studies. *Int. J. Green Energy* **2012**, *9*, 13–21. [[CrossRef](#)]
32. Campo, V.L.; Kawano, D.F.; da Silva, D.B., Jr.; Carvalho, I. Carrageenans: Biological properties, chemical modifications and structural analysis—A review. *Carbohydr. Polym.* **2009**, *77*, 167–180. [[CrossRef](#)]
33. Bosco, M.; Segre, A.; Miertus, S.; Cesaro, A.; Paoletti, S. The disordered conformation of kappa-carrageenan in solution as determined by NMR experiments and molecular modeling. *Carbohydr. Res.* **2005**, *340*, 943–958. [[CrossRef](#)] [[PubMed](#)]
34. Abad, L.V.; Saiki, S.; Nagasawa, N.; Kudo, H.; Katsumura, Y.; De La Rosa, A.M. NMR analysis of fractionated irradiated κ -carrageenan oligomers as plant growth promoter. *Radiat. Phys. Chem.* **2011**, *80*, 977–982. [[CrossRef](#)]
35. Pandey, K.; Asthana, N.; Dwivedi, M.M. Study of structural and conduction behaviour in ionic liquid based polymeric electrolyte membrane with layered filler. *Eur. J. Adv. Eng. Technol.* **2015**, *2*, 96–101.
36. Wan, Y.; Creber, K.A.M.; Peppley, B.; Bui, V.T. Synthesis, characterization and ionic conductive properties of phosphorylated chitosan membranes. *Macromol. Chem. Phys.* **2003**, *204*, 850–858. [[CrossRef](#)]
37. Yamada, M.; Honma, I. Anhydrous proton conductive membrane consisting of chitosan. *Electrochim. Acta* **2005**, *50*, 2837–2841. [[CrossRef](#)]
38. Göktepe, F.; Çelik, S.Ü.; Bozkurt, A. Preparation and the proton conductivity of chitosan/poly(vinyl phosphonic acid) complex polymer electrolytes. *J. Non-Cryst. Solids* **2008**, *354*, 3637–3642. [[CrossRef](#)]
39. Jafirin, S.; Ahmad, I.; Ahmad, A. Potential use of cellulose from kenaf in polymer electrolytes based on MG49 rubber composites. *Bioresources* **2013**, *8*, 5947–5964. [[CrossRef](#)]
40. Savadekar, N.R.; Karande, V.S.; Vigneshwaran, N.; Bharimalla, A.K.; Mhaske, S.T. Preparation of nano cellulose fibers and its application in kappa-carrageenan based film. *Int. J. Biol. Macromol.* **2012**, *51*, 1008–1013. [[CrossRef](#)] [[PubMed](#)]
41. Dissanayake, M.A.K.L.; Jayathilaka, P.A.R.D.; Bokalawala, R.S.P.; Albinsson, I.; Mellander, B.E. Effect of concentration and grain size of alumina filler on the ionic conductivity enhancement of the (PEO)₉LiCF₃SO₃: Al₂O₃ composite polymer electrolyte. *J. Power Sources* **2003**, *119–121*, 409–414. [[CrossRef](#)]

